

## SHOCK AND THERMAL HISTORY OF EQUILIBRATED EUCRITES FROM ANTARCTICA

Akira YAMAGUCHI\*, G. J. TAYLOR<sup>1</sup> and K. KEIL<sup>1</sup>

*Hawai'i Institute of Geophysics and Planetology, School of Ocean and Earth Science and Technology, University of Hawai'i at Manoa, Honolulu, HI 96822, U. S. A.*

*<sup>1</sup>Also associated with the Hawai'i Center for Volcanology*

**Abstract:** We report petrologic observations of seven equilibrated basaltic eucrites from Antarctica. These eucrites are metamorphic rocks (type 4 to 7), as observed for non-Antarctic monomict eucrites. A-881388 and -881467 are unusual; they are granulitic breccias, but portions still preserve vestiges of igneous textures. A-87272 is a coarse-grained rock, containing pyroxenes with remnant Ca-zoning and inversion textures (type 7) and is one of the most shocked eucrites. A-881747 is a typical type 4 and Y-86763 a type 5 eucrite. RKP80204 has very fine-grained, basaltic clasts in which some pigeonites are partially inverted to orthopyroxene due to slow subsolidus cooling (type 6). LEW 86002 is a moderately shocked type 5 eucrite. These rocks cooled rapidly at their liquidus, but orders of magnitude slower at subsolidus temperatures. The most likely heat source for metamorphism is simple burial of a succession of lava flows as the crust grew by extrusive volcanism and intrusions. Heat diffusing from the hot interior of the parent body caused the temperature to rise in the crust, leading to widespread metamorphism. The variety of shock textures observed suggests that impact events were active before, during, and after thermal metamorphism on the asteroid 4 Vesta, the likely eucrite parent body.

### 1. Introduction

Eucrites formed as basaltic lavas that erupted on the surface of an asteroid, presumably 4 Vesta (BINZEL and XU, 1993). This volcanic epoch may have consisted of lava flows, fire fountains, and intrusions of narrow dikes (WILSON and KEIL, 1996) or possibly more global melting that produced a magma ocean (TAYLOR *et al.*, 1993). This period lasted only several million years, as shown by the presence of the decay product of short-lived nuclides in eucrites (*e.g.*, SHUKOLYUKOV and LUGMAIR, 1993). Subsequent impact cratering events produced howardites and polymict eucrites, which mixed eucrites with deeper materials, mainly diogenites.

In spite of the production of vast quantities of volcanic products, a striking feature of eucrites is that almost all of them are metamorphosed (*e.g.*, REID and BARNARD, 1979; TAKEDA and GRAHAM, 1991; YAMAGUCHI *et al.*, 1996a), suggesting a metamorphic event of global proportions. Recently, YAMAGUCHI *et al.* (1996a, 1997) sug-

---

\* Present address: National Institute for Research in Inorganic Materials, 1-1 Namiki, Tsukuba 305.

gested that the thermal history of eucrites simply reflects rapid crustal growth by serial magmatism (STOLPER, 1977; WALKER, 1983). We have been studying the metamorphic record in basaltic eucrites to quantify their metamorphic histories and to understand the geologic evolution of the crust of Vesta.

As was observed for non-Antarctic eucrites (*e.g.*, MASON *et al.*, 1979), monomict eucrites comprise a significant proportion of the Antarctic eucrites (*e.g.*, TAKEDA, 1991; MASON *et al.*, 1992; YANAI, 1993; GROSSMANN, 1994; YANAI and KOJIMA, 1995). Recently, YANAI (1993) identified 5 equilibrated basaltic monomict eucrites (4 from Asuka and 1 from Yamato). Two of them are unusual, showing a granulitic texture. We have examined 7 basaltic eucrites from Antarctica (Table 1), including the 4 Asuka eucrites. These rocks have a variety of metamorphic and shock textures. We focused our study on how textures and mineralogies of basaltic eucrites changed during these secondary processes.

## 2. Samples and Analytical Techniques

The eucrites studied are listed in Table 1. Optical microscopy was performed with a Nikon petrographic photo microscope equipped for transmitted and reflected light. We observed microtextures using a Zeiss DSM 962 scanning electron microscope (SEM). Minerals were analyzed with a Cameca Camebax electron probe microanalyzer (EPMA) operated at an accelerating voltage of 15 kV and absorbed beam current of 20 nA for pyroxene, chromite and ilmenite, and 10 nA for plagioclase and silica minerals. Natural and synthetic phases of well-known compositions were used as standards, and data were corrected using a ZAF program. Modal compositions (Table 2) were determined optically by point counting except for phosphate, which was estimated from PK $\alpha$  imaging. Chemical compositions of minerals are shown in Tables 3–6 and Figs. 1–3. Phases of low-Ca pyroxenes (orthopyroxene and pigeonite) were identified optically.

Table 1. Samples, petrologic types, and equilibration temperatures of the eucrites studied.

Samples <sup>*1</sup>	Split	Petrologic type <sup>*2</sup>	T (°C) <sup>*3</sup>	Remarks
A-87272	71-2	7	815	Highly shocked
A-881388	54-2	–	907	Granulite
A-881467	54-2	–	881	Granulite
A-881747	52-1	4	852	Basaltic
Y-86763	51-2	5	–	Basaltic
RKPA80204	19	6	824	Basaltic (clasts)
LEW86002	16	5	829	Basaltic

<sup>\*1</sup>Asuka (A) and Yamato (Y) are from National Institute of Polar Research;

Reckling Peak (RKPA) and Lewis Cliff (LEW) from Meteorite Working Group, JSC.

<sup>\*2</sup>Petrologic type of eucrites of TAKEDA and GRAHAN (1991).

<sup>\*3</sup>Equilibration temperatures of two pyroxene, using the KRETZ (1982) Ca-thermometer.

Table 2. Modes of the basaltic eucrites studied.

	A-87272 71-2	A-881388 54-2	A-881467 54-2	A-881747 52-1	Y-86763 51-2	LEW86002 16	Eucrite mean <sup>*1</sup>
Pyroxene	56.3	53.8	50.5	49.6	53.9	50.3	51.3 ± 2.6
Plagioclase	40.2	41.3	43.3	45.8	42.0	46.6	43.1 ± 2.1
Silica	2.4	3.9	4.7	3.5	3.3	2.6	4.0 ± 1.5
Ilmenite	0.7	0.2	0.6	1.0	3.3	0.4	0.8 ± 0.3
Chromite	0.3	0.6	0.4	0.1	0.3	tr	0.2 ± 0.2
Troilite	0.1	0.3	0.5	0.1	tr	0.1	0.4 ± 0.3
Fe-metal	tr	tr	tr	nd	tr	nd	tr
Phosphate	tr	0.2	tr	0.3	0.2	tr	0.2 ± 0.1
Fayalite	nd	nd	nd	nd	tr	nd	—
Area (mm <sup>2</sup> )	286.4	113.8	124.4	158.8	77.9	238.8	—

One analyzed step=0.1 mm.

<sup>\*1</sup>Eucrite mean data from DELANEY *et al.* (1984), average of 22 basaltic eucrites; tr=trace (<0.1 vol%); nd=not detected.

Table 3. Chemical compositions (wt%) of pyroxenes in the eucrites studied.

	A-87272		A-881388 <sup>*1</sup>		A-881467		A-871747	
	pig	aug	pig	aug	pig	aug	pig	aug
SiO <sub>2</sub>	49.6	50.9	49.7	50.7	49.3	50.4	49.9	51.1
Al <sub>2</sub> O <sub>3</sub>	0.30	0.89	0.25	0.76	0.22	0.82	0.09	0.61
TiO <sub>2</sub>	0.00	0.28	0.24	0.51	0.13	0.53	0.00	0.16
FeO	35.7	17.1	33.6	17.9	34.0	18.7	35.2	17.0
MnO	0.97	0.46	1.09	0.57	0.97	0.56	0.91	0.39
MgO	11.6	9.95	11.7	9.95	10.9	9.37	11.8	10.3
CaO	1.43	19.9	3.08	18.5	3.92	18.5	2.21	19.6
Cr <sub>2</sub> O <sub>3</sub>	0.03	0.48	0.12	0.28	0.00	0.33	0.01	0.22
Total	99.7	99.9	99.9	99.3	99.5	99.2	100.0	99.4
Wo	3.1	35.6	6.7	39.9	8.6	33.2	4.8	41.6
En	42.3	29.4	35.8	29.9	40.1	28.3	35.5	30.3

	Y-86763 <sup>*2</sup>		RKPA80204		LEW86002	
	pig	aug	pig	aug	pig	aug
SiO <sub>2</sub>	48.7	49.7	49.8	51.3	50.1	51.3
Al <sub>2</sub> O <sub>3</sub>	0.15	1.03	0.14	0.51	0.27	0.79
TiO <sub>2</sub>	1.17	0.71	0.12	0.30	0.12	0.30
FeO	36.8	25.8	34.8	15.8	12.6	10.5
MnO	1.02	0.82	1.10	0.50	1.11	0.50
MgO	11.6	11.0	12.7	10.7	12.6	10.5
CaO	0.82	9.98	1.03	20.2	0.84	19.8
Cr <sub>2</sub> O <sub>3</sub>	0.06	0.38	0.03	0.21	0.16	0.23
Total	100.3	99.4	99.7	99.5	100.4	99.2
Wo	1.8	22.0	2.2	42.6	1.8	42.5
En	35.3	44.3	38.5	31.4	38.2	31.2

<sup>\*1</sup>Bulk chemical compositions of each phase, determined by broad beam analysis (30 μm in diameter).

<sup>\*2</sup>Pigeonite-augite pair with widest Ca-range.

Table 4. Chemical compositions (wt%) of plagioclases in the eucrites studied.

	A-87272	A-881388	A-881467	A-881747		Y-86763	RKPA80204		LEW 86002	
				core	rim		core	rim	core	rim
SiO <sub>2</sub>	45.1	45.7	45.9	45.6	48.3	45.8	45.7	47.3	45.1	49.6
Al <sub>2</sub> O <sub>3</sub>	35.6	35.3	35.0	35.3	33.0	35.0	34.3	34.4	35.8	32.9
FeO	0.23	0.20	0.43	0.20	0.18	0.40	0.71	0.17	0.08	0.07
CaO	18.0	18.1	17.64	17.9	15.6	17.9	17.7	16.8	18.3	15.8
Na <sub>2</sub> O	0.95	1.10	1.20	1.16	2.24	1.08	1.06	1.62	0.97	2.06
K <sub>2</sub> O	0.07	0.12	0.12	0.10	0.29	0.09	0.03	0.18	0.04	0.32
Total	100.4	100.5	100.4	100.2	99.6	100.3	99.5	100.5	100.3	100.7
Or	0.4	0.7	0.7	0.6	1.7	0.5	0.2	1.1	0.2	1.9
Ab	8.7	9.8	10.9	10.5	20.3	9.8	9.8	14.7	8.8	18.8

Table 5. Chemical compositions (wt%) of ilmenites in the eucrites studied.

	A-87272	A-881388	A-881467	A-881747	Y-86763	RKPA80204
SiO <sub>2</sub>	0.00	0.00	0.00	0.00	0.00	0.03
Al <sub>2</sub> O <sub>3</sub>	0.01	0.00	0.00	0.00	0.03	0.05
TiO <sub>2</sub>	53.2	53.1	53.0	53.2	52.9	51.5
FeO	45.2	45.0	44.8	44.5	45.5	44.8
MnO	0.90	0.74	0.72	0.83	1.05	0.98
MgO	0.61	1.07	1.10	1.09	0.37	0.38
CaO	0.04	0.03	0.00	0.04	0.03	0.23
Cr <sub>2</sub> O <sub>3</sub>	0.03	0.09	0.00	0.01	0.28	0.06
Total	99.9	100.0	99.6	99.6	100.2	98.0

Table 6. Chemical compositions (wt%) of spinel in A-881388, A-881467, and Y-86763.

	A-881388		A-881467		Y-86763
	sp1	sp2	sp1	sp2	
SiO <sub>2</sub>	0.03	0.00	0.00	0.00	0.00
Al <sub>2</sub> O <sub>3</sub>	6.96	3.02	5.74	3.39	9.09
TiO <sub>2</sub>	7.22	20.9	10.6	19.7	5.35
FeO	38.7	49.4	41.2	49.5	37.3
MnO	0.56	0.74	0.51	0.60	0.70
MgO	0.75	0.84	0.71	0.83	0.37
CaO	0.05	0.16	0.04	0.02	0.04
Cr <sub>2</sub> O <sub>3</sub>	43.4	22.9	39.9	24.7	47.3
Total	98.2	97.9	98.8	98.8	100.1

### 3. Results

#### 3.1. A-87272

This rock is a highly shocked monomict eucrite (YANAI, 1993; YANAI and KOJIMA, 1995). TAKEDA *et al.* (1996a, b) reported that it is a type 7 eucrite. PTS, A-87272,71-2 has a very heterogeneous texture. One portion (a few mm in size) has elongated angular to irregular plagioclase (or maskelynite) ( $0.4 \times 2$ – $1.2 \times 1.6$  mm) and highly

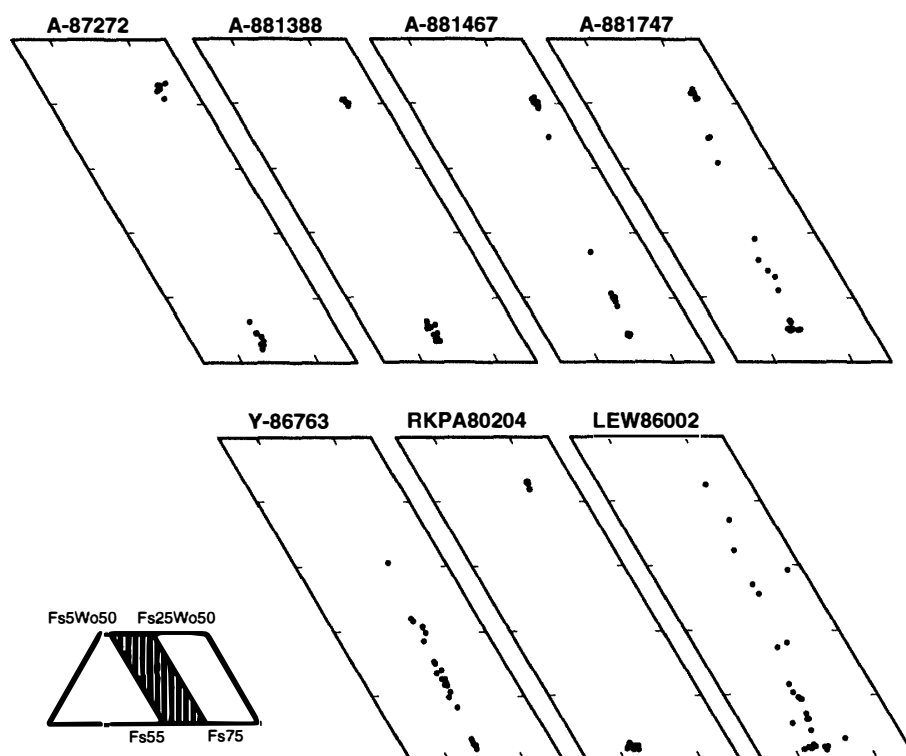


Fig. 1. Chemical compositions of pyroxenes in the eucrites studied. Intermediate compositions between low- and high-Ca pyroxenes are due to incomplete resolution of electron probe.

fractured pyroxenes ( $1.2 \times 1.6$  mm) (Fig. 4a and b); other portions of this rock have granulitic textures ( $40\text{--}80$   $\mu\text{m}$  in diameter). There are several relict mesostasis areas containing large, irregular silica ( $\sim 150 \times 100$   $\mu\text{m}$ ) and oxide minerals (mainly ilmenites) up to  $500$   $\mu\text{m}$  in size. Other minor minerals include troilite and Fe-metal and terrestrial weathering products.

The pyroxenes show exsolution textures with coarsely spaced ( $70\text{--}60$   $\mu\text{m}$  apart), thick augite lamellae ( $\sim 40$   $\mu\text{m}$  thick) and fine lamellae along (100) with distances of  $<3\text{--}6$   $\mu\text{m}$  between them. These augite lamellae are the thickest among basaltic eucrites, similar to those observed in LEW88005 (YAMAGUCHI *et al.*, 1996a). Pigeonite hosts are partially inverted to ortho pyroxene. As described by TAKEDA *et al.* (1996a, b), some pyroxenes have remnant Ca-zoning in which augite lamellae are concentrated in the rim. There are two types of remnant Ca-zoning in A-87272; bundles ( $\sim 100 \times 300$   $\mu\text{m}$ ) of thin augite lamellae located along the rim but not in the core, and dense augite lamellae ( $\sim 10$   $\mu\text{m}$  thick) decreasing its thickness toward the core. Cloudy pyroxenes are not common. Dusty inclusions (mainly oxides,  $10\text{--}30$   $\mu\text{m}$  in size) are located along healed cracks, sometimes forming worm-shaped inclusions ( $30 \times 3$   $\mu\text{m}$ ). Occasionally, minute opaque pellets ( $<1 \times 10$   $\mu\text{m}$ ) are aligned in certain crystallographic orientations of the pyroxenes. Irregular to angular plagioclase inclusions are common ( $10\text{--}80$   $\mu\text{m}$  in size) in the pyroxenes. Chemical compositions of the pyroxenes are  $\text{Wo}_{40.6-43.1}\text{En}_{28.4-30.1}$  (augites) and  $\text{Wo}_{1.9-4.4}\text{En}_{35.5-36.4}$  (pigeonites) (Table 3, Fig. 1). Most of the plagioclases are maskelynitized (Fig. 4b) (see below). The plagioclase crystals are general-

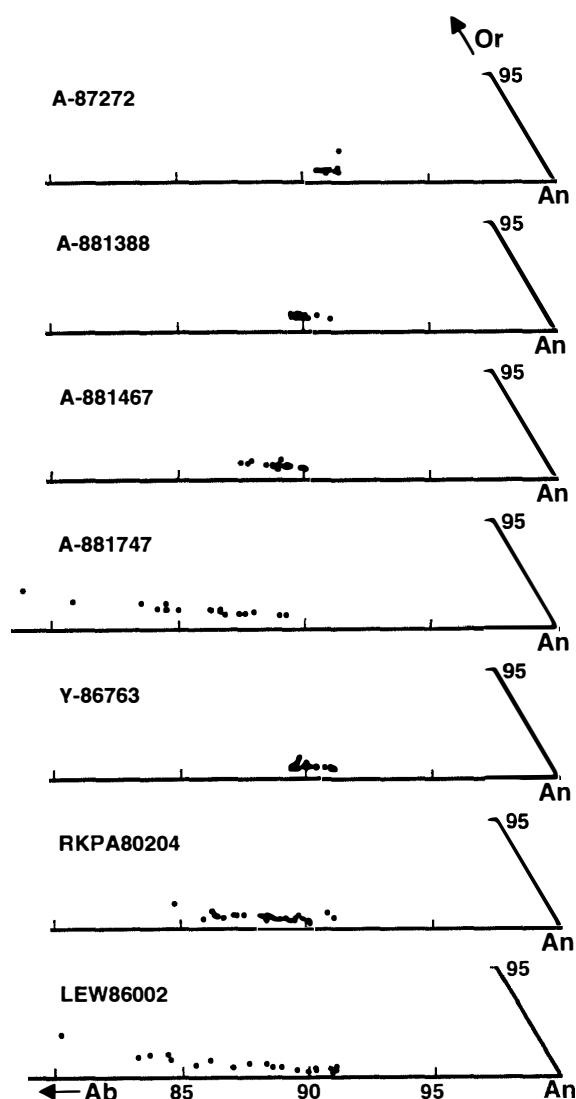


Fig. 2. Chemical compositions of plagioclases in the eucrites studied.

ly clear, but some have a cloudy appearance due to the presence of small pyroxene and silica inclusions. Plagioclases are quite uniform in composition ( $An_{90.4-91.3}$ ) (Table 4 and Fig. 2). Ilmenite, often associated with chromite, is common. Sometimes, the oxide minerals contain tiny plagioclase and pyroxene inclusions. Silica minerals are finely recrystallized (or fractured?) and contain a significant amount of  $K_2O$  (0.07–0.22 wt%).

A-87272 appears to be one of the most severely shocked eucrites. This rock is slightly crushed, but still preserves the original (igneous and metamorphic) textures to some extent. Fracturing of minerals is very common, especially along the boundaries of the minerals. The PTS is crossed by several thin, dark microfaults, forming a network. Pyroxene displays a pervasive, strong mosaicism (Fig. 4c). Some mosaic domains are elongated roughly parallel to the (001) plane. In both augite and pigeonite, there are dense planar features parallel to the c-axis of the crystals, but it is difficult to identify them because of the presence of fine lamellae along (100) (see above). The (001) exsolution boundaries between augite and pigeonite are often wavy, perhaps due

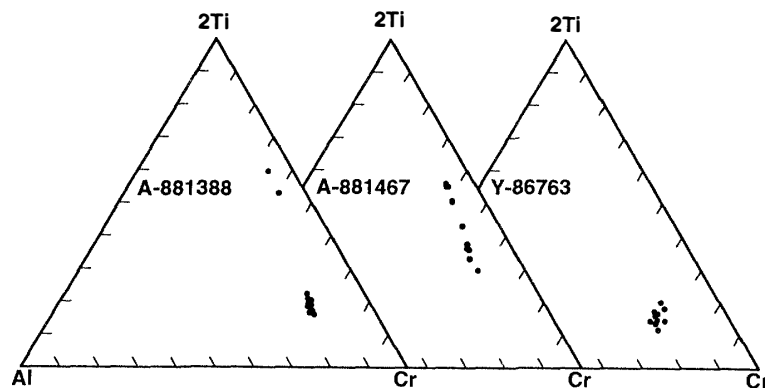


Fig. 3. Chemical compositions of spinels in A-881388, A-881467, and Y-86763.

to shock deformation. In contrast to the pyroxenes, the plagioclase crystals are remarkably unfractured. However, about 40 vol% of the plagioclases are converted into maskelynite, and the rest of the crystals are finely recrystallized or have prominent wavy extinction. Although highly shocked, the presence of mosaicism in the plagioclase is not obvious. Most ilmenite crystals are fractured and contain very fine twin lamellae (1–3  $\mu\text{m}$  in width).

### 3.2. A-881388 and A-881467

A-881388 and A-881467 are unusual in having recrystallized textures (YANAI, 1993; YAMAGUCHI *et al.*, 1996b) (Fig. 5a, b). They consist mainly of granules of pigeonite, augite and plagioclase (30–200  $\mu\text{m}$ ; average  $\sim 100$   $\mu\text{m}$  in diameter), and minor minerals (ilmenite, chromite, troilite and silica minerals), with well-developed  $120^\circ$  triple junctions and curved boundaries (Fig. 6). There is little ambiguous remnant igneous texture; some plagioclases occur as laths from  $\sim 900 \times 200$  to  $300 \times 60$   $\mu\text{m}$  in size (Fig. 5b), which may be vestiges of the original igneous texture. Opaque minerals ( $\sim 80$   $\mu\text{m}$  in size), such as ilmenite and chromite, are scattered evenly throughout the thin sections. Silica minerals ( $< 200$   $\mu\text{m}$ ) occur interstitial to pyroxene and plagioclase and are lath or irregularly shaped (Fig. 6). Although mesostasis is not clearly observed in the PTSs, there are a few granular assemblages ( $500 \times 500$   $\mu\text{m}$ ) of silica minerals, pyroxene, plagioclase, oxides, and troilite, which may be relict mesostasis.

The pyroxenes are pigeonite and augite (Fig. 6), as observed in recrystallized portions in many eucrites (YAMAGUCHI *et al.*, 1996a). The pigeonites contain very fine-grained, closely spaced (2–3  $\mu\text{m}$  in width) augite lamellae ( $< 1$ –2  $\mu\text{m}$  thick), but the separate augite grains appear to have less common inclusions or exsolved phases. Pyroxenes (Table 3, Fig. 1) in A-881388 are slightly more magnesian than those in A-881467. Clouding in the pyroxenes is rare. Most plagioclase grains are clear, but contain pyroxene fragments ( $\sim 20$ –50  $\mu\text{m}$  in size). Some plagioclases have a cloudy appearance due to the presence of fine needles ( $< 5 \times 2$   $\mu\text{m}$ ) of pyroxene and a silica mineral. Compositional ranges of plagioclases are narrow and the meteorites have slightly different ranges (A-881388:  $\text{An}_{89.2-90.9}$ ; A-881467:  $\text{An}_{87.1-89.8}$ ) (Table 4, Fig. 2). In both meteorites, ilmenite is often associated with chromite and rarely with troilite

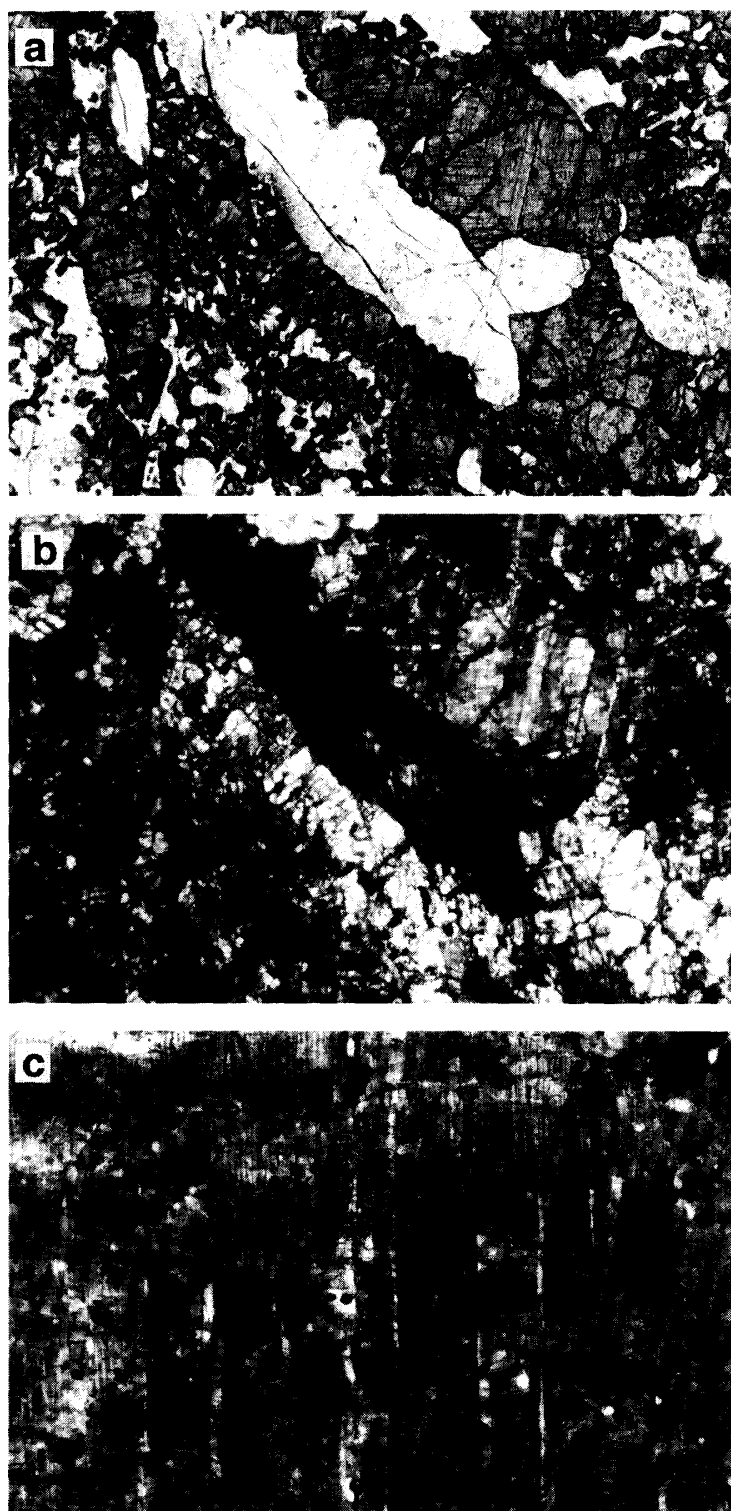


Fig. 4. Photomicrograph of A-87272,71-2 (a). Image (b) shows the same texture in cross-polarized light. Width is 2.6 mm. Plagioclases are mostly converted into maskelynite; a core portion of the elongated plagioclase (middle) is finely recrystallized. Notice that the texture is very heterogeneous. (c) A strongly mosaicized pyroxene. Cross-polarized light. Width = 0.3 mm.

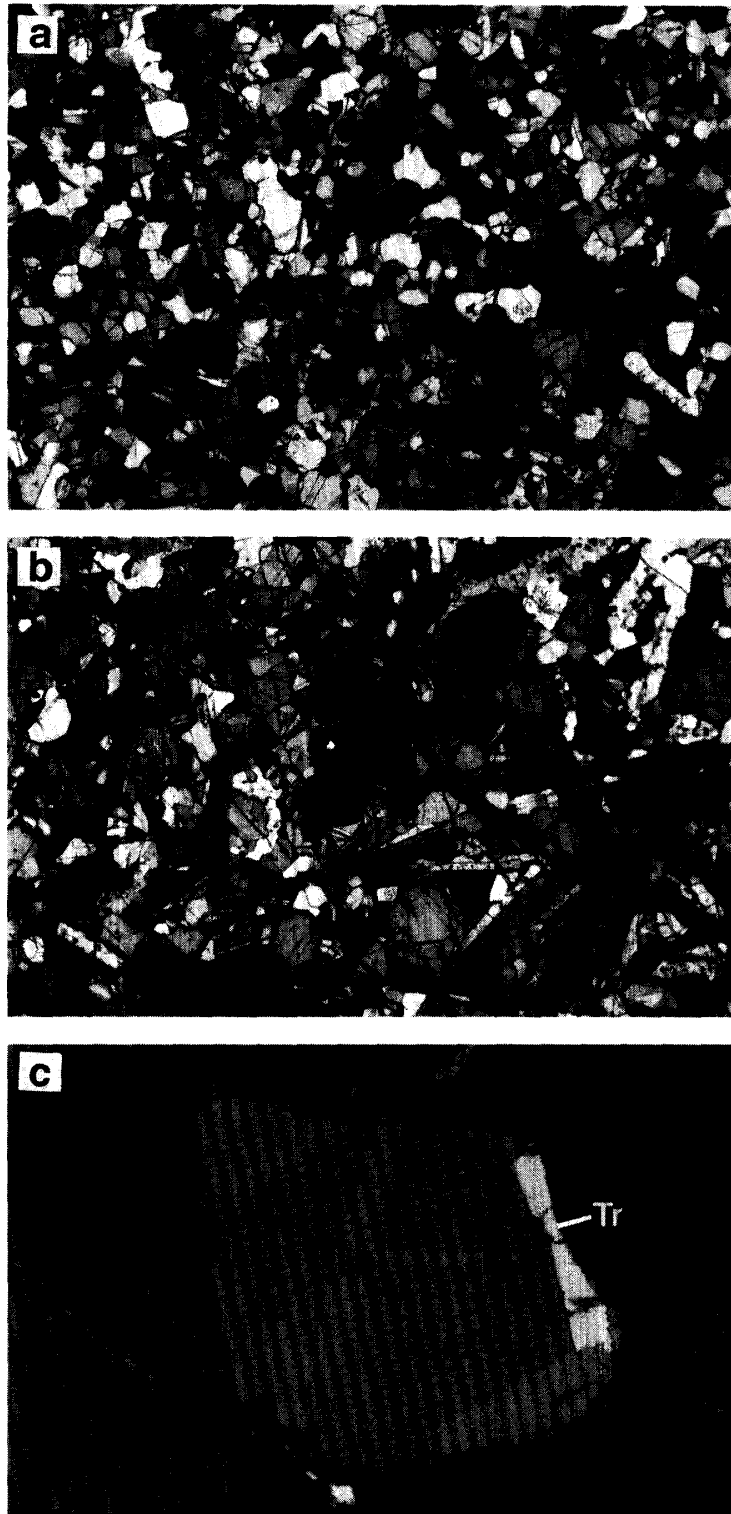


Fig. 5. Photomicrograph of A-881388,54-2 (a) and A-881467,54-2 (b), showing granulitic textures. Widths are 2.6 mm. Partially polarized. In A-881467 (b), there are several plagioclase laths, which may be the vestige of original igneous texture. (c) Image of opaque grain, composed of lamellae of ilmenite (Im; light gray) in a chromite grain (Cm; middle gray in the middle) and tiny, elongated troilite (Tr; white). Reflected light. Width = 130  $\mu$ m.

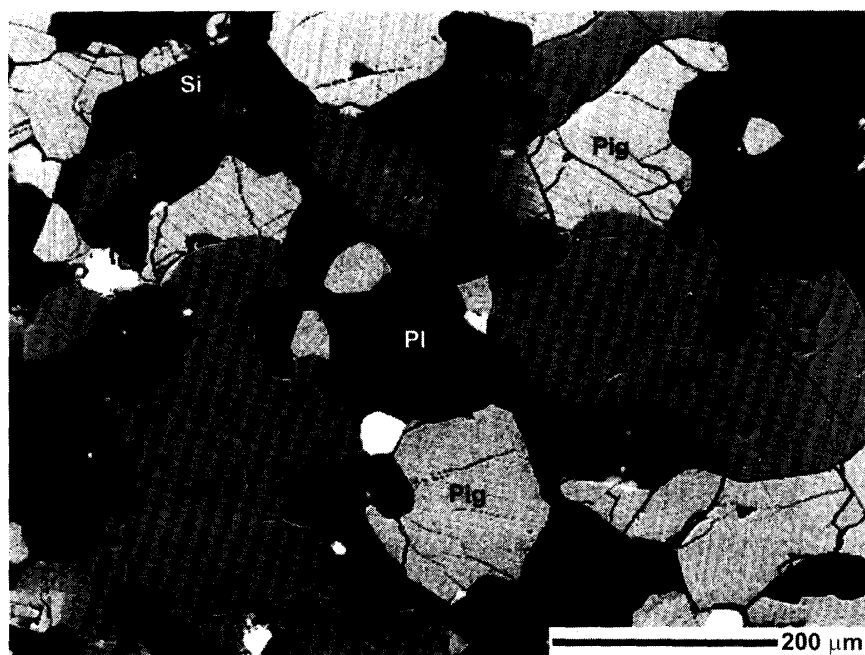


Fig. 6. Backscattered electron image (BEI) of A-881388,54-2, showing granulitic texture. This image indicates that this rock contains two pyroxenes, augite (Aug; medium gray) and pigeonite (Pig; light gray). Dark gray=plagioclase (Pl); black=silica mineral (Si); white=opaque minerals.

(Fig. 5c).  $\text{Cr}_2\text{O}_3$  contents in ilmenites of A-881388 are variable from 0.09–1.3 wt%, but those in A-881467 are less than 0.7 wt%. Chromite in A-881388 appears to be composed of high Ti- and low Ti-chromite (Fig. 3), like those in Ibitira (STEELE and SMITH, 1976).

These rocks are unbrecciated and show slight fracturing. Many plagioclases and pyroxenes show very sharp extinction, but some show very weak mottled extinction in which misorientations inside the single crystals are less than  $5^\circ$ .

### 3.3. A-881747

PTS A-881747,52-1 displays a subophitic texture, consisting of coarse, lath-shaped plagioclase ( $<2.9 \times 0.8$  mm) and anhedral, irregular pyroxene ( $\sim 1.7 \times 0.6$  mm in size) (Fig. 7a). The rock appears to be slightly crushed but preserves its original igneous texture. Large oxide ( $\sim 400 \times 200$   $\mu\text{m}$  in size) minerals (mainly ilmenites) are distributed randomly in the PTS. Minor minerals include ilmenite, chromite, troilite and Fe-metal.

Most pyroxenes are aggregates that consist of very fine, randomly-oriented crystals sizes varying from 20 to 100  $\mu\text{m}$ ; a few crystals are fairly large ( $0.55 \times 0.6$  mm) and are surrounded by the brecciated pyroxenes. The pyroxene crystals show remnant Ca-zoning (Fig. 8), with rims of closely spaced thick ( $\sim 10$   $\mu\text{m}$  thick) augite lamellae and cores with sparsely ( $\sim 50$ – $100$   $\mu\text{m}$  in width) spaced augite lamellae ( $\sim 10$   $\mu\text{m}$  thick); such eucrites are classified as type 4 (TAKEDA and GRAHAM, 1991). Pyroxenes compositions plot along a single tie line in the quadrilateral from  $\text{Wo}_{4.8}\text{En}_{35.5}$  to  $\text{Wo}_{41.6}\text{En}_{30.3}$

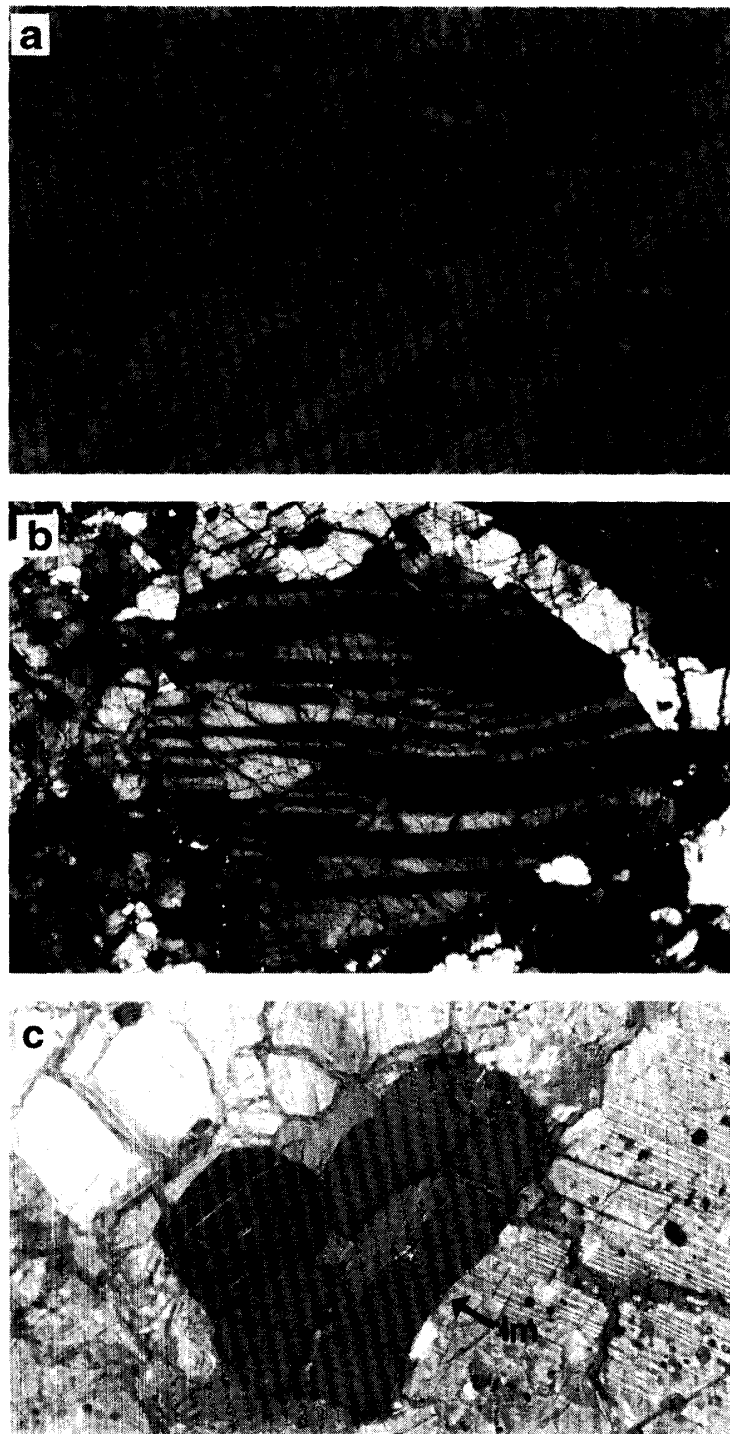


Fig. 7. Photomicrograph of A-881747,52-1. (a) Overall view. Width = 2.6 mm. Both pyroxene and plagioclase show cloudy features. (b) Strongly deformed plagioclase in crossed polarized light. Width = 1.3 mm. (c) Reflected image of ilmenite grain (Im, dark in the middle), containing fine twin lamellae. Width = 0.3 mm.

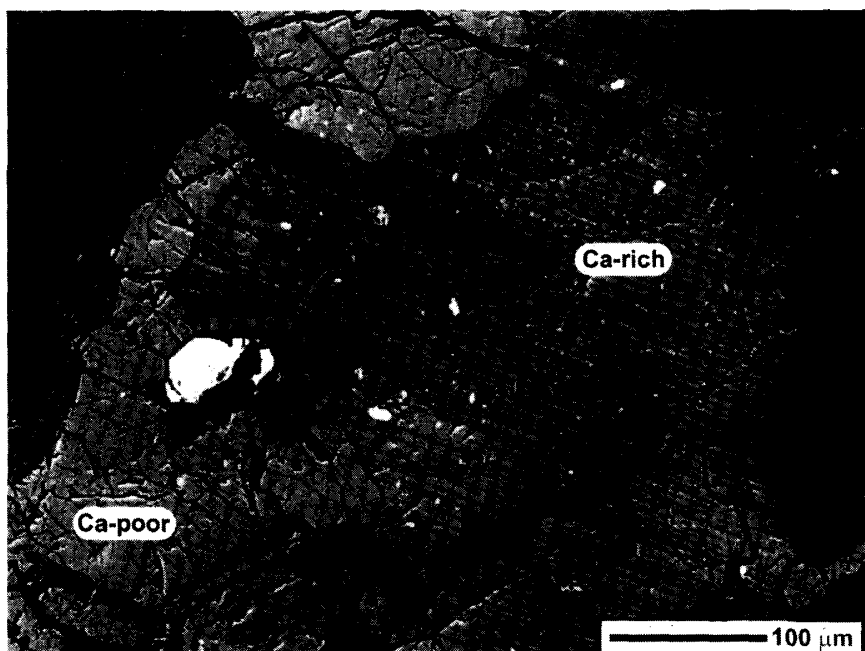


Fig. 8. BEI of A-881747,52-1. The image shows remnant Ca-zoning, in which density of augite lamellae (medium gray) changes from left to right. Dark gray=plagioclase; white=opaque minerals.

(Table 3, Fig. 1). The large pyroxene crystals have dense clouding due to the presence of tiny inclusions of opaques (mainly chromite and ilmenite) and plagioclase. Finer ( $<1\text{--}2\ \mu\text{m}$  in size) opaque inclusions tend to have needle-like shapes, whereas coarse ( $1\text{--}5\ \mu\text{m}$  in size) ones are sub-rounded. Sometimes, narrow plagioclase veins ( $5\text{--}8\ \mu\text{m}$  in width) are observed in the brecciated pyroxenes. Smaller pyroxenes, on the other hand, are not cloudy. Plagioclase in A-881747 is compositionally zoned from  $\text{An}_{89.0}\text{Or}_{0.59}$  to  $\text{An}_{78.0}\text{Or}_{1.7}$  (Fig. 2, Table 4), a trend similar to those observed in unequilibrated eucrites (*e.g.*, Pasamonte clasts). Plagioclase crystals are cloudy except near the boundaries with the pyroxene crystals. The cloudy phases are mainly fine ( $<1\ \mu\text{m}$ ) pigeonites and silica minerals and rarely oxide minerals and troilite-metal. The silica minerals mainly occur at the boundaries between pyroxene and plagioclase crystals. Ilmenites often contain closely-spaced fine ( $\sim$  a few  $\mu\text{m}$  thick) lamellae, which probably are mechanical twins (STÖFFLER *et al.*, 1986), because they show no compositional differences to the ilmenite host (Fig. 7c). Troilite is often replaced by terrestrial weathering products. A few Fe-rich olivines grains (*e.g.*,  $40 \times 20\ \mu\text{m}$ ) are observed and are associated with the oxide minerals. There are several tiny (several  $\mu\text{m}$  in size) Fe-metal grains in this PTS.

This rock was moderately shocked. The pyroxene crystals are fractured and show weak mosaicism. Each domain is elongated ( $\sim 15 \times 8\ \mu\text{m}$  in size) roughly parallel to the (001) plane, as observed in A-87272 (see above). The plagioclase crystals are highly fractured and show strong mottled extinction. Weak mosaicism is observed in a few crystals. The twin boundaries in the plagioclase are deformed and crushed (Fig. 7b). In contrast to the pyroxene grains, plagioclase grains still preserve large single crys-

tals, although their outlines are deformed.

### 3.4. Y-86763

Y-86763,51-2 is a small thin section, outlined by a dark-colored fusion crust. This rock is a subophitic eucrite consisting of lathy plagioclase ( $<0.8 \times 0.4$  mm) and anhedral to granular pyroxene ( $\sim 0.8 \times 0.4$  mm) (Fig. 9). This portion of the eucrite appears to be unbrecciated and only minor fracturing is observed. Mesostasis is finely recrystallized. Boundaries of the minerals are curved, and edges of plagioclase laths are rounded, as observed in the strongly metamorphosed eucrite, EET 90020 (YAMAGUCHI *et al.*, 1996b). Minor minerals include oxides (ilmenite and chromite), troilite, Fe-metal and Fe-rich olivine. This rock is weakly shocked; pyroxene and plagioclase show very weak mottled extinction.

The pigeonite crystals contain closely spaced ( $\sim 1\text{--}5$   $\mu\text{m}$ ) very thin augite lamellae ( $<1$   $\mu\text{m}$ ) which are homogeneously distributed; this rock is a type 5 eucrite (TAKEDA and GRAHAM, 1991). The pyroxene crystals are very clear but show minor clouding. Some areas in the pyroxene contain rounded to elongated, fine ( $<10$   $\mu\text{m}$  in size) opaque inclusions; more rarely they contain Fe-rich olivine grains. Near the fusion crust, the pyroxenes are dirty because of the presence of minute troilite droplets in the cracks and the cleavages. Chemical compositions of pyroxenes vary from  $\text{Wo}_{1.8}\text{En}_{35.3}$  to  $\text{Wo}_{30.6}\text{En}_{32.4}$  (Fig. 1; Table 3). The apparent low Ca-contents of augite (Table 3) are an artifact and are due to incomplete resolution of electron probe analytical spots (*ca.* 2  $\mu\text{m}$ ). Most of the plagioclases are clear; some crystals are cloudy due to the presence fine inclusions. Three types of inclusions are observed; relatively large (6–30  $\mu\text{m}$ ), subrounded pyroxenes, plate-like pyroxenes ( $3 \times 60\text{--}10 \times 40$   $\mu\text{m}$  in size), and irregular to subrounded inclusions of a silica mineral (tridymite?). The inclusions of a silica mineral are often observed adjacent to the recrystallized mesostasis. The narrow compositional range of plagioclase from  $\text{Or}_{0.4}\text{Ab}_{8.7}$  to  $\text{Or}_{0.5}\text{Ab}_{10.3}$  suggests partial equi-



Fig. 9. Photomicrograph of Y-86763,51-2. Plane light. Width=2.6 mm.

libration (Fig. 2, Table 4). Ilmenite grains are common, and chromites are less common than ilmenite and are associated with them. A few oxide minerals have thin rims ( $\sim$  several  $\mu\text{m}$  in width) of Fe-rich olivine along the boundary with pyroxenes, similar to those in Ibitira (STEELE and SMITH, 1976).

### 3.5. RKPA 80204

RKPA 80204 is a brecciated eucrite, containing two lithologies (MASON and CLARKE, 1982; SCORE *et al.*, 1984). PTS, 19 is a crushed (monomict-like) rock mainly composed of very fine-grained clasts with minor clastic matrix, crossed by impact melt veins ( $<100 \mu\text{m}$  in width). We could not find the coarse-grained lithology reported by SCORE *et al.* (1984) in this section (.19). The fine-grained basalts are composed of anhedral to granular pyroxene ( $\sim 600 \times 200 \mu\text{m}$ ), plagioclase laths ( $\sim 300 \times 50 \mu\text{m}$ ), and minor fine ( $10\text{--}20 \mu\text{m}$  in size), subrounded ilmenite and chromite (Fig. 10a). These clasts are texturally quite similar to FX-clasts in Millbillillie (YAMAGUCHI *et al.*, 1994).

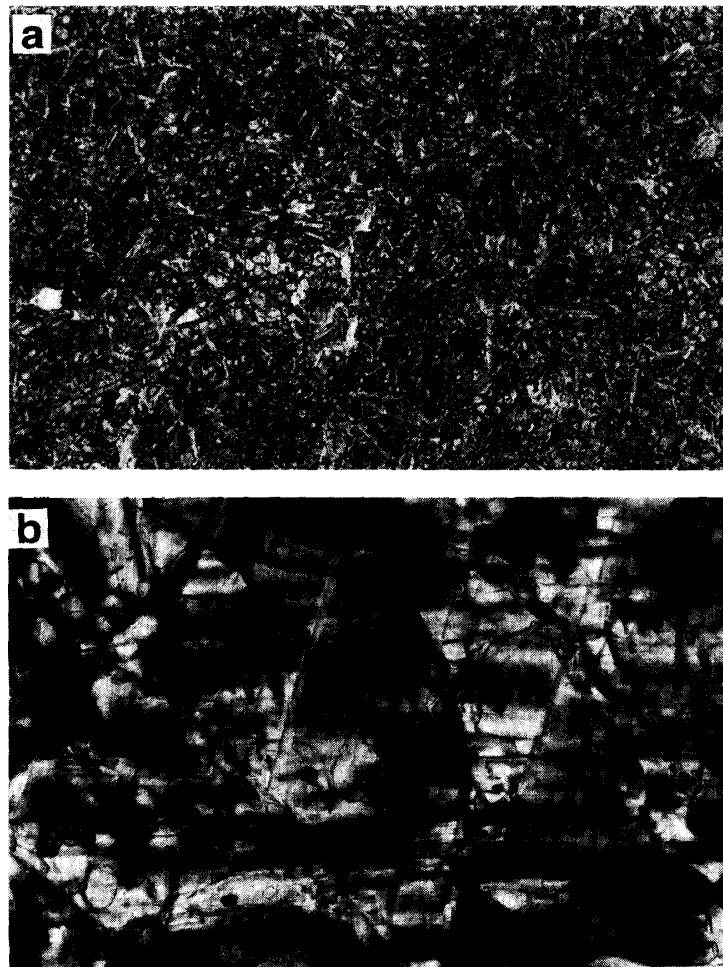


Fig. 10. Photomicrograph of RKPA80204,19. (a) Overall view, showing very fine-grained basaltic texture. (b) Partly inverted pigeonite. Black horizontal streaks are portions of orthopyroxenes. Cross polarized light. Width = 0.3 mm.

Rare troilite grains are distributed randomly, but are often associated with silica minerals where large rusty features are observed (mesostasis?). Irregular silica minerals occur interstitially between the plagioclase laths. Rare Fe-metal grains (less than 5  $\mu\text{m}$ ) also occur.

The pyroxene consists of pigeonite hosts with thin (001) augite lamellae. Some pigeonites are partially inverted to orthopyroxene in which very fine (100) augite lamellae ( $<1 \mu\text{m}$ ) are located between thicker (001) augite lamellae (7–20  $\mu\text{m}$  thick) (Fig. 10b). This suggests that RKP 80204 is a type 6 eucrite (TAKEDA and GRAHAM, 1991). Pyroxenes are very homogeneous (Fig. 1, Table 3), and pyroxene crystals are clear but often contain visible inclusions of oxide minerals. Plagioclases are chemically zoned from  $\text{An}_{90.9}\text{Or}_{0.40}$  to  $\text{An}_{84.2}\text{Or}_{1.07}$  (Fig. 2, Table 4) and plagioclase laths contain fine inclusions of pyroxene and silica minerals, as observed in other eucrites.

As reported by SCORE *et al.* (1984), this PTS contains minor impact melt veins. Pyroxene crystals show strong mosaic and mottled extinction (misorientation  $\sim 15^\circ$ ). Some plagioclases are strongly crushed and show strong mottled extinction. Portions of some plagioclases are converted to maskelynite.

### 3.6. LEW 86002

LEW 86002, 16 is an unbrecciated rock with an ophitic intergrowth of pyroxene and plagioclase (MASON *et al.*, 1992). It is composed of anhedral large pyroxenes (0.8  $\times$  1 mm) and finer plagioclase laths (400  $\times$  40–550  $\times$  10  $\mu\text{m}$ ) (Fig. 11a). Large, angular ilmenite grains ( $<350 \mu\text{m}$ ) occur randomly. Mesostasis regions ( $\sim 1$  mm in size) are finely recrystallized and composed of a silica mineral, pyroxene, plagioclase, ilmenite, chromite and troilite (all  $\sim 5$ –10  $\mu\text{m}$ ).

The pyroxene is pigeonite, containing closely spaced (1–5  $\mu\text{m}$ ) augite lamellae ( $<1 \mu\text{m}$ ) and has brownish clouding due to the presence of fine opaque inclusions similar to Juvinas (TAKEDA and YAMAGUCHI, 1991). Pyroxenes are homogeneous, and compositions are scattered along the augite-pigeonite tie line (Fig. 1, Table 3). Thus, this rock is a typical type 5 eucrite. Some irregular plagioclase veins (*e.g.*, 3  $\times$  90  $\mu\text{m}$ ) intruded into the pyroxenes. Portions of the pyroxenes are irregularly replaced by granular crystals ( $\sim 10 \mu\text{m}$ ) (see below). The plagioclases show normal chemical zoning ( $\text{An}_{91.0}\text{Or}_{0.2}$ – $\text{An}_{79.3}\text{Or}_{1.9}$ ) (Fig. 2, Table 4) and contain sparse, dusty inclusions of pyroxene and silica minerals. Some of the pyroxene inclusions are shaped like pellets ( $\sim 1 \times 20 \mu\text{m}$ ). Ilmenite is the third most abundant mineral and often occurs with chromite grains. Ilmenite has fine mechanical twinning and a few ilmenites contain plates of chromites.

This rock is moderately shocked. Minor fracturing and veins are common. The pyroxene crystals show strong mottled extinction, and some show mosaic features in which misorientation in the single crystal is  $\sim 40^\circ$ . These pyroxenes are often replaced by fine ( $\sim 10 \mu\text{m}$  in size), granular crystals (Fig. 11b, c); the clouding is wiped out and oxide minerals occur as discrete, larger grains (several  $\mu\text{m}$  in size). In spite of the recrystallization, original igneous boundaries are preserved. Some pyroxenes have planar features. The exsolution lamellae in augite are wavy due to deformation. The plagioclase crystals are strongly fractured and deformed and show strong mottled extinction. Small anisotropic portions are commonly observed in the plagioclases.

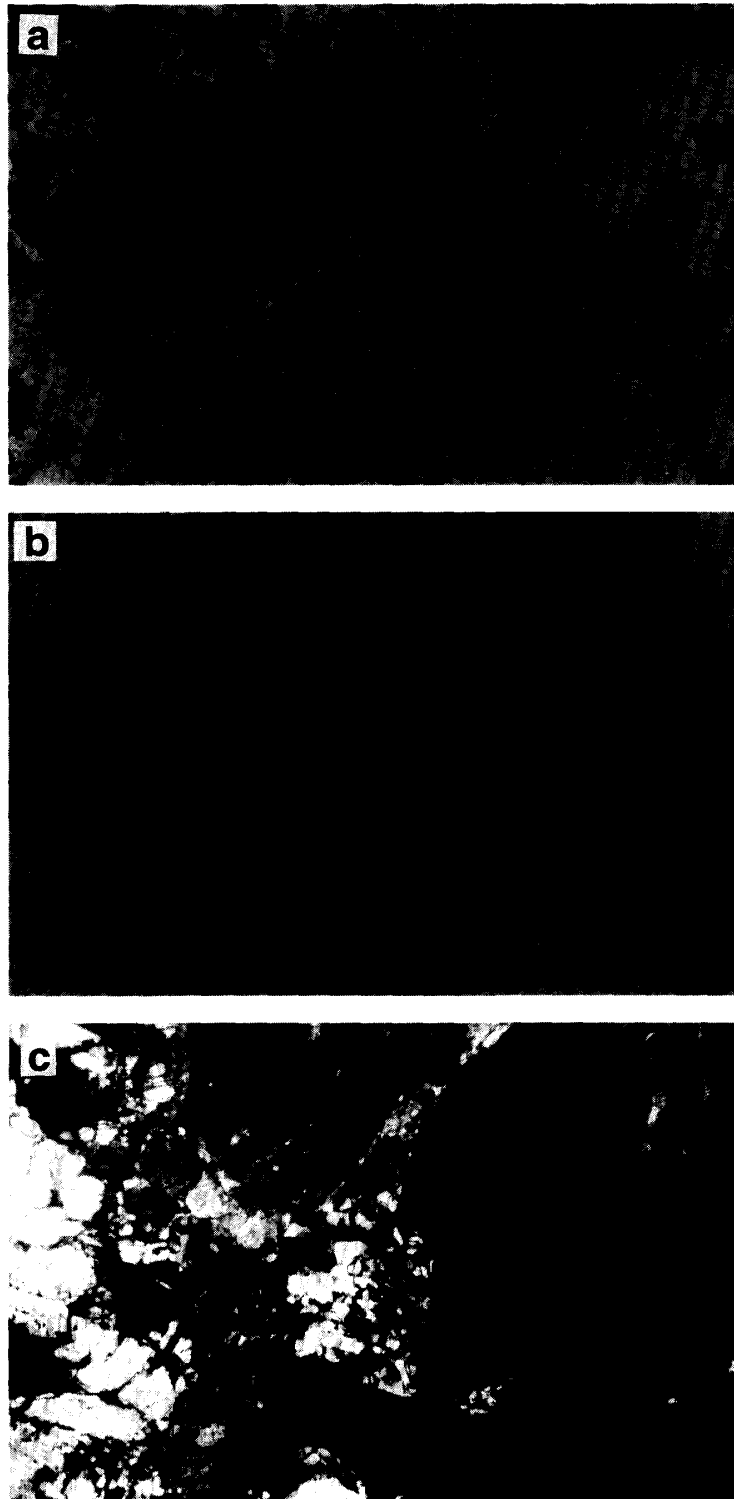


Fig. 11. Photomicrograph of LEW 86002,16. (a) Overall view, showing subophitic texture. Images (b) (plane light) and (c) (crossed polarized light) show a portion of granular pyroxenes (Gp). Width = 0.6 mm. Notice that portions of pyroxene are recrystallized, while the lath shape of plagioclase (lower-middle) is preserved.

## 4. Discussion

### 4.1. Classification

On the basis of the mineralogical features such as FeO/MnO ratios of pyroxenes and modal abundances (Table 2), there is no doubt that these rocks are eucrites. A-881388 and A-881467 are unusual, and we classify them as granulitic breccias. In spite of the fact that these meteorites have similar petrographic features, slight differences in the pyroxene and the plagioclase compositions suggest that they might not be paired (Figs. 1, 2). A-881388, A-881747 and Y-86763 have been classified as cumulate eucrites (YANAI and KOJIMA, 1995), but the modal abundances of these eucrites are comparable to those in ordinary basaltic eucrites. However, the bulk chemical composition of A-881388 is slightly enriched in  $\text{Al}_2\text{O}_3$  (13.86 wt%) (YANAI and KOJIMA, 1995), compared to other basaltic eucrites ( $\text{Al}_2\text{O}_3$  ~12–13 wt%, MASON *et al.*, 1979). Measurement of trace elements of these eucrites is required to resolve this classification puzzle.

### 4.2. Shock effects in eucrites

The eucrites we studied have various shock textures, including undulatory extinction and mosaicism in pyroxene and plagioclase, planar features in pyroxene and ilmenite, and maskelynitization of plagioclase. There are also pervasive fractures (minor brecciation) and impact melt veins (microfaults) present. These observations suggest that shock stages of the rocks range from 0–2a, implying equilibrium shock pressures up to 28–34 GPa, based on the classification by STÖFFLER *et al.* (1988). As discussed below, these shock effects modified the original igneous textures.

STÖFFLER *et al.* (1986) suggested that isotropization of plagioclase occurs at shock pressure of ~26 GPa and plagioclase totally converts to maskelynite at greater than about 28 GPa for a plagioclase of  $\text{An}_{80}$ . In A-87272, plagioclases (~ $\text{An}_{91}$ , Fig. 2) are mostly converted to maskelynite, suggesting equilibrium shock pressures of about ~26–28 GPa. The presence of pervasive, strong mosaicism in the pyroxenes is consistent with this shock pressure estimate (BISCHOFF and STÖFFLER, 1992). A-87272 is unusual among eucrites because of the presence of maskelynite; other eucrites like A-87272 include Padvarninkai (YAMAGUCHI *et al.*, 1993) and ALHA 81313 (DELANEY and PRINZ, 1989); plagioclases in ALHA 81313 have totally converted to maskelynite (our unpublished data) in contrast to those in A-87272 and Padvarninkai (YAMAGUCHI *et al.*, 1993). Incomplete isotropization of plagioclases in A-87272 and Padvarninkai could be due to a short duration of reheating or slow cooling after shock; maskelynites easily recrystallize as a result of short duration of reheating (*e.g.*, 1 hr at 1000°C, OSTERTAG and STÖFFLER, 1982).

Several workers have discussed the importance of shock effects in pyroxene in basaltic eucrites. Cloudy features in pigeonites are very common in equilibrated basaltic eucrites (*e.g.*, A-881747 and LEW 85002). This is due to the presence of tiny precipitates of minor minerals (mainly chromite). HARLOW and KLIMENTIDIS (1980) and MORI and TAKEDA (1985) suggested that planar fractures that may have been formed by shock events acted as favorable nucleation sites for chromites in pigeonites. Transformation of pigeonites may be related to shock metamorphism (MORI and

TAKEDA, 1988). Dislocations parallel to the c-axis may have acted as nucleation sites for orthopyroxene layers in pigeonites. Clearly, the planar features in pigeonite and augite in A-87272 and the associated wavy (001) augite lamellae were produced by shock deformation. So, it might be possible that the partial inversion textures in A-87272 and RKPA 80204 could be due to shock effects, as proposed by MORI and TAKEDA (1988). However, although almost all eucrites contain shock effects (*e.g.*, METZLER *et al.*, 1995; YAMAGUCHI *et al.*, 1996a), inversion textures large enough to be observed by optical microscopy are relatively uncommon in basaltic eucrites (YAMAGUCHI *et al.*, 1996a). In other words, the shock textures are not always associated with the inversion textures. This suggests that shock may not be the cause of the inversion. Because coarsening of orthopyroxene layers require prolonged periods of annealing, it is likely that inversion took place during a metamorphic event (see below).

In igneous textured regions of LEW 86002, some portions of pyroxenes are replaced by unshocked, fine granular pyroxene crystals (Fig. 11). In contrast, similar recrystallization textures are absent in the highly shocked eucrite A-87272. In the case of olivine, recrystallization to form tiny granular crystals up to  $\sim 10 \mu\text{m}$  along healed cracks or locally fractured regions can easily occur during a short reheating event (BAUER, 1979). Thus, it is likely that the recrystallization texture in LEW 86002 was formed by post-shock annealing. The clouding (due to submicron size opaque minerals) of the recrystallized regions were locally wiped out, forming larger oxide grains ( $\sim 100 \mu\text{m}$  in size). This texture is commonly observed, for example, in Juvinas (TAKEDA and YAMAGUCHI, 1991), Y-74356 (YAMAGUCHI and TAKEDA, 1995) and A-881388 and -881467 (this work), although the textures are more coarsely ( $\sim$  tens  $\mu\text{m}$  in size) recrystallized and the igneous textures are erased. The texture in LEW 86002 is the initial stage of the recrystallization process recorded in Juvinas and other eucrites.

#### 4.3. *Thermal history of eucrites and implications for the evolution of the crust of the eucrite parent body*

The features in the eucrites described here and in other eucrites can be used to explore the thermal history of the crust of the eucrite parent body. As shown in Table 1, petrologic type (TAKEDA and GRAHAM, 1991; YAMAGUCHI *et al.*, 1996a) varies; A-881747: type 4; Y-86763 and LEW 86002: type 5; clasts in RKPA 80204: type 6; and A-87272: type 7. The equilibration temperatures of augites and pigeonites (KRETZ, 1982) range from 820–880°C (Table 1), which are far below the solidus temperature of eucrites ( $\sim 1060^\circ\text{C}$ , STOLPER, 1977), suggesting that these eucrites experienced sub-solidus annealing.

Many workers have pointed out that the most abundant type of basaltic eucrites are metamorphosed to varying degrees. REID and BARNARD (1979) classified eucrites into two types; equilibrated and unequilibrated eucrites. Based on the detailed pyroxene mineralogy, TAKEDA and GRAHAM (1991) have characterized the metamorphic degree of basaltic eucrites from types 1–6; a type 7 eucrite has been proposed by YAMAGUCHI *et al.* (1996a). It should be noted that the TAKEDA-GRAHAM classification from types 4–7 is based only on the pyroxene mineralogy in igneous portions, so it does not always completely represent the degree of annealing. YAMAGUCHI *et al.* (1996a) have attempted to interpret the TAKEDA-GRAHAM classification, assuming

monotonous slow cooling from a peak temperature. They suggested that each type of eucrite experienced a separate thermal history with respect to peak temperature and cooling rate (or metamorphic time scale). Types 4 and 7 experienced relatively low peak temperatures (~800–1000°C), as shown by the presence of remnant Ca-zoning. Types 5 and 6 do not have remnant Ca-zoning in pigeonite, thus they annealed at a higher temperature close to or above the two-pyroxene solvus (~1000°C). The presence of the partly inverted pigeonite suggests that the metamorphic time scale of types 6 and 7 may be longer than that of types 4 and 5 (see below).

The mechanisms of exsolution and inversion of pigeonites in eucrites have been described in detail (ISHII and TAKEDA, 1974). If primary pigeonites of basaltic eucrites cooled very slowly in the subsolidus regime, they would transform into orthopyroxene in a complex way, resulting in Stillwater-type pyroxenes (ISHII and TAKEDA, 1974). Although RKPA80205 clasts have fine-grained basaltic textures, the pigeonites in them are partially inverted to orthopyroxene, as are those observed in the Moore County cumulate eucrite. Compared to Moore County, the partly inverted pigeonites in the basaltic eucrites have much more closely spaced and finer (001) lamellae. Furthermore, many cumulate eucrites have completely inverted pigeonites. However, this may not have been caused simply by differences in the cooling rates, because inversion and exsolution may be affected by various factors such as compositions of the pyroxenes. For example, bulk Mg/(Mg+Fe) of the pyroxene in Moore County is high; thus, the inversion and exsolution of pyroxenes in this cumulate eucrite may have taken place at a higher temperature (ISHII and TAKEDA, 1974) with consequent faster diffusion, so exsolution and inversion might have occurred more effectively. If so, the cooling rates of some basaltic eucrites might have been similar to those of cumulate eucrites.

Most eucrites are overprinted by secondary processes (METZLER *et al.*, 1995; YAMAGUCHI *et al.*, 1996a, b; this work). For example, the granulitic breccias (YAMAGUCHI and TAKEDA, 1994, 1995; this work) may be formed by recrystallization of brecciated basaltic eucrites. Metamorphic phases such as augite and chromite were produced during the annealing (see below). Eucritic granulites are common in breccia clasts in howardites and mesosiderites (*e.g.*, FUHRMAN and PAPIKE, 1981) and in parts of the equilibrated basaltic eucrites (YAMAGUCHI *et al.*, 1996a), but rarely as whole meteorites. As discussed above, the A-881388 and -881467 are coarser granulites than those previously reported, and formed by more extensive annealing. LEW 85305 is similar (DELANEY, 1987).

Some other minerals were also affected by thermal metamorphism. For example, Na-Ca zoning in plagioclase is notoriously resistant to thermal metamorphism. However, the Ibitira plagioclase has little compositional variation, probably due to annealing (STEELE and SMITH, 1976). Similarly, plagioclases in some eucrites studied here (*e.g.*, A-87272, -881388, and Y-86763, Fig. 2) have very narrow compositional ranges, also suggesting intense annealing. Another notable feature is the occurrence of oxide minerals. The close relationship between ilmenite and chromite, which is sometimes an exsolution relationship, is often observed in many type 5 eucrites such as Ibitira (STEELE and SMITH, 1976), LEW85305 (DELANEY, 1987), Y-74356 (YAMAGUCHI and TAKEDA, 1995), and A-881388 (this work; TAKEDA *et al.*, 1996a). This oxide assemblage could have formed during thermal metamorphism. TAKEDA *et*

*al.* (1996a) suggested that the A-881388 oxides formed below 800°C. HARLOW and KLIMENTIDIS (1980) suggested that fine oxide minerals were formed from incompatible elements such as Ti and Cr incorporated into pyroxenes during rapid initial cooling. Since some ilmenites (with high Mn/Cr) may be the major carrier of  $^{53}\text{Cr}$  (NYQUIST *et al.*, 1996), the origin of these phases are important for dating the metamorphic ages of eucrites.

As discussed above, many eucrites cooled very slowly below the solidus, implying that they resided in hot environments, yet they formed initially by rapid cooling in thin lava flows (*e.g.*, YAMAGUCHI *et al.*, 1996a). What geological history led to the extensive metamorphism of a series of lava flows? The rocks are extensively brecciated and shocked as well, so one might argue that the metamorphism could have been caused by impact heating. However, the metamorphism is ubiquitous among eucrites and it may have lasted thousands to millions of years (MIYAMOTO *et al.*, 1985; YAMAGUCHI *et al.*, 1996a), implying that metamorphism was very widespread. Such metamorphism requires extensive heating of a huge cooling mass and very slow cooling and, thus, it is impossible to achieve by impact processes (KEIL *et al.* 1996). In fact, if anything, impacts probably cooled the crust by excavating hot rocks buried at depth. The most likely source of the heat for metamorphism, therefore, is simple burial of a succession of lava flows as the crust grew by volcanism and intrusions (YAMAGUCHI *et al.*, 1996a). In this model, lava flows initially on top would be buried progressively deeper and heated by internal heat. Notice that direct heat from molten lavas on the surface cannot be the heat source for metamorphism, because the cooling time of an individual lava flow (~1 yr) is much smaller than the interval between eruptions at any given site, assuming reasonable eruption rates on Vesta (*e.g.*, 18 km<sup>3</sup>/yr, YAMAGUCHI *et al.*, 1996a, 1997).

Textural evidence suggests that most eucrites experienced shock metamorphism and brecciation events before, during and after metamorphism (*e.g.*, METZLER *et al.*, 1995; this work). In the scenario described above (YAMAGUCHI *et al.*, 1996a), lava flows originally at the top surface would be easily brecciated by frequent small cratering events. These impact events would produce regolith and monomict breccias. These brecciated materials would be progressively buried by subsequent lava flows. After the volcanism, the entire hot crust, which is composed of brecciated lava flows (eucrites) and regolith, would have cooled very slowly to closure temperatures of pyroxenes (700–1000°C, YAMAGUCHI *et al.*, 1996a), producing recrystallized breccias (*e.g.*, eucritic granulites such as A-881388). Intense meteorite bombardment of Vesta, on the other hand, could have continued long after the volcanic and metamorphic events for more than 1 Ga (BOGARD, 1995), producing a variety of shocked rocks and breccias. Large cratering events would excavate deep material or brecciate *in situ* most of the deeply buried (thus, strongly metamorphosed) rocks.

### Acknowledgments

We thank the National Institute of Polar Research (NIPR) and the Meteorite Working Group for the loan of meteorite thin sections. We thank H. TAKEDA and E. R. D. SCOTT for discussions, T. HULSEBOSCH, G. BENEDIX and D. MCGEE for techni-

cal assistance, and M. MIYAMOTO and D. W. MITTFELDLT for thoughtful reviews. This work was supported by NASA Grant NA65-4212 (K. KEIL, P. I.). This is Hawai'i Institute of Geophysics and Planetology Publication No. 963 and School of Ocean and Earth Science and Technology Publication No. 4542.

### References

- BAUER, J. F. (1979): Experimental shock metamorphism of mono- and polycrystalline olivine: A comparative study. *Proc. Lunar Planet. Sci. Conf.*, 10th, 2573–2596.
- BINZEL, R. P. and XU, S. (1993): Chips off of asteroid 4 Vesta: Evidence for the parent body of basaltic achondrite meteorites. *Science*, **260**, 186–191.
- BISCHOFF, A. and STÖFFLER, D. (1992): Shock metamorphism as a fundamental process in the evolution of planetary bodies: Information from meteorites. *Eur. J. Mineral.*, **4**, 707–755.
- BOGARD, D. D. (1995): Impact ages of meteorites: A synthesis. *Meteoritics*, **30**, 244–268.
- DELANEY, J. S. (1987) The Lewis Cliff 85305 eucrite, and shock effects in eucrites. *Meteoritics*, **22**, 365–366.
- DELANEY, J. S. and PRINZ, M. (1989): Overview of some achondrite groups. *Smithson. Contrib. Earth Sci.*, **28**, 65–79.
- FUHRMANN, M. and PAPIKE, J. J. (1981): Howardites and polymict eucrites; Regolith samples from the eucrite parent body. Petrology of Bholghati, Bununu, Kapoeta and ALHA76005. *Proc. Lunar Planet. Sci. Conf.*, 12B, 1257–1280.
- GROSSMAN, J. N. (1994): The meteoritical bulletin, No. 76, 1994 January: The U.S. Antarctic Meteorite Collection. *Meteoritics*, **29**, 100–143.
- HARLOW, G. E. and KLIMENTIDIS, R. (1980): Clouding of pyroxenes and plagioclase in eucrites: implication for post-crystallization processing. *Proc. Lunar Planet. Sci. Conf.*, 11th, 1131–1143.
- ISHII, T. and TAKEDA, H. (1974): Inversion, decomposition and exsolution phenomena of terrestrial and extraterrestrial pigeonites. *Mem. Geol. Soc. Jpn.*, **11**, 19–36.
- KEIL, K., STÖFFLER, D., LOVE, S. G., and SCOTT, E. R. D. (1996): Constraints on the role of impact heating and melting in asteroids. *Meteoritics*, **31**, A69–A70.
- KRETZ, R. (1982): Transfer and exchange equilibria in a portion of the pyroxene quadrilateral as deduced from natural and experimental data. *Geochim. Cosmochim. Acta*, **46**, 411–421.
- MASON, B. and CLARKE, Jr., R. S. (1982): Characterization of the 1980-81 Victoria Land meteorite collections. *Mem. Natl Inst. Polar Res., Spec. Issue*, **25**, 17–33.
- MASON, B., JAROSEWICH, E. and NELEN, J. A. (1979): The pyroxene-plagioclase achondrites. *Smithson. Contrib. Earth Sci.*, **22**, 27–45.
- MASON, B., MCPHERSON, G. J., SCORE, R., MARTINEZ, R., SATTERWHITE, C., SCHWARZ, C., and GOODING, J. L. (1992): Description of stony meteorites. *Smithson. Contrib. Earth. Sci.*, **30**, 17–35.
- METZLER, K., BOBE, K.-D., PALME, H., SPETTEL, B. and STÖFFLER, D. (1995): Thermal and impact metamorphism of the HED parent body. *Planet. Space Sci.*, **43**, 499–525.
- MIYAMOTO, M., DUKE M. B. and MCKAY D. S. (1985): Chemical zoning and homogenization of Pasamonte-type pyroxene and their bearing on thermal metamorphism of Howardite parent body. *Proc. Lunar Planet. Sci. Conf.*, 15th, Pt. 2, C629–C635 (*J. Geophys. Res.*, **90** Suppl.).
- MORI, H. and TAKEDA, H. (1985): Oriented chromite inclusions in pigeonite crystals of eucrite meteorites. Papers Presented to the 10th Symposium on Antarctic Meteorites, March 25-27, 1985. Tokyo, Natl Inst. Polar Res., 26–28.
- MORI, H. and TAKEDA, H. (1988): Stress induced transformation of pigeonites from achondritic meteorites. *Phys. Chem. Mineral.*, **15**, 252–259.
- NYQUIST, L. E., TAKEDA, H., BOGARD, D. D., SHIH, C.-Y. and WIESMANN, H. (1996): Crystallization, recrystallization, and impact metamorphic ages of monomict eucrite Y792510. *Lunar and Planetary Science XXVII*. Houston, Lunar Planet. Inst., 969–970.
- OSTERTAG, R. and STÖFFLER, D. (1982): Thermal annealing of experimentally shocked feldspar crystals. *Proc. Lunar Planet. Sci. Conf.*, 13th, Pt. 1, A457–A463 (*J. Geophys. Res.*, **87** Suppl.), .
- REID, A. M. and BARNARD, B. M. (1979): Unequilibrated and equilibrated eucrites. *Lunar and Planetary*

- Science X. Houston, Lunar Planet. Inst, 1019–1021.
- SCORE, R., SHWARZ, C. M. and MASON, B. (1984): Description of stony meteorites. *Smithson. Contrib. Earth Sci.*, **26**, 23–47.
- SHUKOLYUKOV, A. and LUGMAIR, G. W. (1993): Live iron-60 in the early solar system. *Science*, **259**, 1138–1141.
- STEELE, I. M. and SMITH, J. V. (1976): Mineralogy of the Ibitira eucrite and comparison with other eucrites and lunar samples. *Earth Planet. Sci. Lett.*, **33**, 67–78.
- STÖFFLER, D., OSTERTAG, R., JAMMES, C., PFANNSCHMIDT, G., SEN GUPTA, P. R., PAPIKE, J. J. and BEAUCHAMP, R. H. (1986): Shock metamorphism and petrography of the Shergotty achondrite. *Geochim. Cosmochim. Acta.*, **50**, 889–903.
- STÖFFLER, D., BISCHOFF, A., BUCHWALD, V. and RUBIN, A. E. (1988): Shock effects in meteorites. *Meteorites and the Early Solar System*, ed. by J. F. KERRIDGE. Tucson, Univ. Arizona Press, 165–202.
- STOLPER, E. (1977): Experimental petrology of eucritic meteorites. *Geochim. Cosmochim. Acta*, **41**, 587–611.
- TAKEDA, H. (1991): Comparison of Antarctic and non-Antarctic achondrite and possible origin of the difference. *Geochim. Cosmochim. Acta*, **55**, 35–47.
- TAKEDA, H. and GRAHAM, A. L. (1991): Degree of equilibration of eucritic pyroxenes and thermal metamorphism of the earliest planetary crust. *Meteoritics*, **26**, 129–134.
- TAKEDA, H. and YAMAGUCHI, A. (1991): Recrystallization and shock textures of old and new samples of Juvinas in relation to its thermal history. *Meteoritics*, **26**, 400.
- TAKEDA, H., ISHII, T., ARAI, T. and MIYAMOTO, M. (1996a): Mineralogy of Asuka 87 and 88 eucrites and crustal evolution of the eucrite parent body. *Antarctic Meteorites XXI*. Tokyo, Natl Inst. Polar Res., 170–173.
- TAKEDA, H., ISHII, T. and MIYAMOTO, M. (1996b): Coarsely exsolved pyroxenes in a eucrite from Antarctica and the highest degree of crustal metamorphism. *Meteoritics*, **31**, A138–A139.
- TAYLOR, G. J., KEIL, K., MCCOY, T., HAACK, H. and SCOTT, E. R. D. (1993): Asteroid Differentiation: Pyroclastic volcanism to magma ocean. *Meteoritics*, **28**, 34–52.
- WALKER, D. (1983): Lunar and terrestrial crust formation. *Proc. Lunar Planet. Sci. Conf.*, 14th, Pt. 1, B17–B25 (*J. Geophys. Res.*, **88** Suppl.).
- WILSON, L. and KEIL, K. (1996): Volcanic eruptions and intrusions on the asteroid 4 Vesta. *J. Geophys. Res., Planet.*, **101**, 18927–18940.
- YAMAGUCHI, A. and TAKEDA, H. (1994): Granulitic matrices in monomict eucrites. *Lunar and Planetary Science XXV*. Houston, Lunar Planet. Inst., 1525–1526.
- YAMAGUCHI, A. and TAKEDA, H. (1995): Mineralogical study of some Antarctic monomict eucrites including Yamato 74356—A unique rock containing recrystallized clastic matrix. *Proc. NIPR Symp. Antarct. Meteorites*, **8**, 167–184.
- YAMAGUCHI, A., MORI, H. and TAKEDA, H. (1993): Mineralogy and shock textures in the Padvaminkai eucrite. *Meteoritics*, **28**, 462–463.
- YAMAGUCHI, A., TAKEDA, H., BOGARD, D. D. and GARRISON, D. H. (1994): Textural variation and impact history of the Millbillillie eucrite. *Meteoritics*, **29**, 237–245.
- YAMAGUCHI, A., TAYLOR, G. J. and KEIL, K. (1996a): Global crustal metamorphism of the eucrite parent body. *Icarus*, **124**, 97–112.
- YAMAGUCHI, A., TAYLOR, G. J. and KEIL, K. (1996b): Three unbrecciated eucrites: Global metamorphism on the eucrite parent body. *Lunar and Planetary Science XXVII*. Houston, Lunar Planet. Inst., 1469–1470.
- YAMAGUCHI, A., TAYLOR, G. J. and KEIL, K. (1997): Metamorphic history of the eucritic crust of 4 Vesta. *J. Geophys. Res.*, **102**, 13381–13386.
- YANAI, K. (1993): The Asuka-87 and Asuka-88 collections of Antarctic meteorites: Preliminary examination with brief description of some typical and unique-unusual specimens. *Proc. NIPR Symp. Antarct. Meteorites*, **6**, 148–170.
- YANAI, K. and KOJIMA, H. comp. (1995): *Photographic Catalog of the Antarctic Meteorites*. Tokyo, Natl Inst. Polar Res., 230 p.

(Received August 9, 1996; Revised manuscript accepted January 20, 1997)